Available online at www.sciencedirect.com

SciVerse ScienceDirect

Procedia IUTAM 8 (2013) 257 – 266

Procedia IUTAM

www.elsevier.com/locate/procedia

IUTAM Symposium on Waves in Fluids: Effects of Nonlinearity, Rotation, Stratification and Dissipation

Diffusion Induced Flows on a Strip: Theoretical, Numerical and Laboratory Modeling

Iaroslav V. Zagumennyi [a,*], Yuli D. Chashechkin [b]

[a] *Institute of Hydromechanics NAS of Ukraine, Zhelyabov str., Kiev 03680, Ukraine*
[b] *Institute for Problems in Mechanics of the RAS, pr. Vernadskogo, Moscow 119526, Russia*

Abstract

Non-stationary problem of a diffusion-induced flow around a motionless sloping plate submerged in a quiescent continuously stratified fluid is solved using numerical approaches. Breaking of a natural diffusion flux on the impermeable surface leads to deficiency and excess of the stratifying agent above and under the obstacle, respectively, and formation of the compensating fluid flows including basic along-slope jet flows and a complex system of secondary circulating cells. The numerical results are compared with the asymptotic evaluations in the infinite plane approximation and the Schlieren images of stratified flows in the laboratory experiments, which visualize extensive horizontal streaky structures generated by extreme points of the motionless obstacles.

Keywords: continuosly stratified fluid; diffusion; flow finestructure; circulating cells; dissipative gravitational waves; numerical modeling; Schlieren visualization

1. Introduction

Nowadays among the most urgent unsolved practical and ecological problems there are prediction of wave-nature destructions which cause the most noticeable damage to the world's economy, improvement of aerohydrodynamical properties of moving objects with the purpose of cost-effective energy consumption, monitoring of passive admixtures transport in environmental systems for air and water pollution control, as well. A responsible role in these problems solving is given to mathematical methods of adequate physical modeling, which is constrained to account for the real properties of environmental fluids and effects of external dynamical factors. Mostly due to an essential progress in information technologies during the last decades it has become a reality carrying out numerical simulations of rather complicated problems with a high resolution level of flows finestructure.

* Corresponding author. Tel.: +38-044-453-2662; fax: +38-044-455-6432.
E-mail address: zagumennyi@gmail.com

doi:10.1016/j.piutam.2013.04.032

The environmental systems (the Earth's atmosphere and hydrosphere) and fluids in technological devices are mostly non-homogeneous in space and variable in time due to non-uniform distributions of dissolved or suspended matters, gas bubbles, temperature, medium compressibility and the influence of external forces. Fluid density variations, even though quite weak, give rise to a number of effects absent in homogeneous media including specific types of waves and a medium fine structure.

A stably stratified fluid, which is formed due to the combined influence of medium non-homogeneity and the Earth's gravitation or rotation, is known to be a thermodynamically non-equilibrium system. In turn it gives rise to fluid motions even in the absence of purely mechanical reasons. Among such phenomena are convective flows driven by spatial variations in fluid density or the so-called diffusion-induced flows (DIFs) on topography. A DIF occurs when molecular flux of the substance existing naturally in a stably stratified fluid encounters a sloping boundary (geometrical irregularities of topography) that creates a physical basis for the formation of compensating fluid motions even in an initially quiescent medium. A fluid adjacent to the sloping boundary differs in density from a fluid at the same level away from the boundary, and experiences a buoyancy force that drives the flow up- or down-slope for the underlying and overlying walls, respectively, the kinetic energy of motion being drawn from the internal energy of the fluid through diffusion [1].

A variety of physical processes are triggered by DIFs, including mineral transport in rocks [2, 3], the melting of icebergs [4] and the migration of tectonic plates [5]. Hillside flows formed in both stratified and globally rotating fluids influence strongly the processes of transport of passive substances to a great distance, mixing and formation of a medium fine structure [6, 7]. The action of density gradients, which give rise to jet flow formation along impermeable sloping surfaces causes intensive valley and mountain winds in a stably stratified atmosphere [1,8] and density flows in the ocean [9].

A permanent interest in the problem is maintained by the enlarging spectrum of practical applications including ecological and biological ones. It was revealed that a DIF may trigger propulsion mechanism leading to self-movement of neutral buoyancy solids with a special shape in a continuously stratified ocean medium. The laboratory experiments by Allshouse [10, 11] show that a neutrally buoyant wedge starts to float towards its tip when immersed in a density-stratified fluid due to a macroscopic sideways thrust at its sloping boundaries generated by molecular diffusion. Computer simulations reveal that the thrust results from the DIF creating a region of low pressure at the front, relative to the rear of an object. This discovery has implications for transport processes in regions of varying fluid density, such as marine snow aggregation at ocean pycnoclines [12], and wherever there is a temperature difference between immersed objects and the surrounding fluid, such as particles in volcanic clouds [13]. DIFs, having influence on the displacement of separate elements of plankton, may be maintained both by the breaking of the natural molecular flux of the stratifying agent and additional concentration gradients generated by the products of the natural metabolism of the elementary organisms.

The first mathematical model of DIFs was created in the middle of the past century with application to the problem on mountain and valley winds [1]. The marked universality mechanism of hillside flows formation both in the stratified atmosphere and the ocean [2, 3] restored the interest in the problem after a long pause. In the pioneering theoretical investigations of DIFs the stationary solutions were obtained in the infinite plate approximation on the basis of a linearized system of equations [1]. For constant slope, and assuming along-slope flow that is a function only of the wall-normal coordinate ζ (that is, unidirectional flow), the velocity profile for a steady DIF is $u(\zeta) = u_0 e^{-\gamma\zeta}\sin(\gamma\zeta)$, where $u_0 = 2\kappa_S\gamma\cot\varphi$ is the characteristic tangential flow velocity, $\gamma^{-1} = (N^2\sin^2\varphi / 4\nu\kappa_S)^{-1/4}$ is the along-slope flow thickness, $N = \sqrt{-(g/\rho_0)/(d\rho/dz)}$. The non-stationary problem was analyzed first asymptotically on an infinite slope in [14] and was then solved exactly in [15]. In relation to theoretical aspects, Page and Johnson [16] extended the analysis of Phillips and Wunsch [2, 3] for a semi-infinite fluid to the steady laminar flow of a contained fluid when the induced density perturbation at the boundary is small relative to the background density. First, their governing equations were linear, which assisted them in the determining the flow structure and solutions but the theory was not strictly applicable to practical situations. Subsequently, the analysis was extended to circumstances where the background density gradient

was significantly affected by the motion, and the governing equations were nonlinear. That enabled the results to be compared directly with those of Woods [17] for flow in a V-shaped container, as well as to more general configurations for a contained steady flow.

It is well known that concentration and temperature gradients in marine environment may have different orientations at a general stable density distribution. Presence of additional parameter having influence upon medium density complicates essentially flow structure and dynamics. Computational results show that hillside jet flows may be directed either up- or down-slope in dependence on values of kinetic coefficients and parameters of stratification [18]. Under certain conditions the regime of finger-shaped convection may be formed in the boundary layers over infinite sloping plane.

Calculated patterns of a valley wind arising in a continuously stratified medium over a cold strip being placed on infinite sloping plane are presented in [19]. The obtained results reveal basic downslope jet flow with adjacent much less intensive backflow being formed along the sloping cold strip. The edges of the strip generate two virtually horizontal jets due to compensating drawing of surrounding fluid to the sloping surface, separation and shifts of the main jet flow. The flow pattern turns to be qualitatively similar to that on an impermeable sloping plate in a stratified fluid, where the outgoing jets are surrounded by a system of dissipative gravitational waves [20, 21].

Formation of multiscale flow pattern in the whole space including vicinities of the poles i.e. the extreme upper and lower points of an impermeable sphere immersed in a salinity-stratified fluid, were analyzed numerically in [22]. However a parametric investigation of the solution was not conducted in full content due to the computational complexity of the problem in 3D formulation. Since studying of DIF's finestructure is of a great scientific and practical interest it is more expedient to carry out such an investigation in 2D formulation, which is much simpler for a numerical realization.

In the present paper new results are offered on full numerical investigation of transient dynamics and fine structure of 2D DIF on an impermeable plate immersed in a continuously stratified fluid. The details of the flow patterns are studied both in the direct vicinity of the obstacle where the non-linear effects are essential and at great distances from the plate. Influence of the determining parameters are traced i.e. values of stratification, kinetic coefficients and angular position of the strip, as well. The constructed fields of the flow parameters are compared with the well-known analytical solutions and Schlieren visualization images of the flows being formed around a motionless sloping plate in the laboratory tank.

Nomenclature

(x, y, z)	laboratory coordinate system
(ξ, ς, ζ)	local coordinate system
$\mathbf{v}$	velocity vector
P	pressure perturbation
S	total salinity
s	salinity perturbation
ν	kinematic viscosity
κ_S	molecular diffusivity
$\mathbf{g}$	gravitational acceleration
ρ_0	characteristic fluid density
Λ	stratification scale
T_b, N	buoyancy period and frequency
L	plate's length
φ	slope angle to horizon

2. Governing equations and numerical realization

In order to analyze DIF around a sloping plate numerically we consider the fundamental set of equations including the non-stationary Navier – Stokes accounting for the gravity in the Boussinesq approximation, the continuity and diffusion equations and the closing linearized state equation

$$\frac{\partial \mathbf{v}}{\partial t}+\left(\mathbf{v}\cdot\nabla\right)\mathbf{v}=-\frac{1}{\rho_0}\nabla P+\nu\Delta\mathbf{v}-s\mathbf{g}$$
$$\operatorname{div}\mathbf{v}=0,\quad \frac{\partial s}{\partial t}+\mathbf{v}\cdot\nabla s=\kappa_S\Delta s+\frac{\upsilon_z}{\Lambda},\quad \rho=\rho_0\left(1-\frac{z}{\Lambda}+s\right) \tag{1}$$

At the initial moment of time $t=0$ a thin impermeable plate AB with length L is placed into a quiescent stratified fluid at an angle φ to the horizon without introducing any mechanical disturbances. The laboratory coordinate system $\left(x0z\right)$ and the local one $\left(\xi 0\zeta\right)$ connected to the sloping plate are shown in Fig. 1 along with the typical profiles of longitudinal component of velocity $\upsilon_\xi\left(0,\zeta\right)$ and salinity perturbation $s\left(0,\zeta\right)$ in the center of the plate. The physically valid initial and boundary conditions are zero perturbations before the initial moment of time, no-slip and no-flux boundary conditions for velocity components and salinity on the plate surface, correspondingly, and attenuation of all perturbations at infinity:

$$\mathbf{v},\ s\big|_{t\le 0}=0,\ \upsilon_x\big|_\Sigma=\upsilon_z\big|_\Sigma=0 \tag{2}$$
$$\left[\frac{\partial S}{\partial \mathbf{n}}\right]_\Sigma=-\frac{1}{\Lambda}\frac{\partial z}{\partial \mathbf{n}}+\left[\frac{\partial s}{\partial \mathbf{n}}\right]_\Sigma=0,\ \mathbf{v},\ s\big|_{x,\,z\to\infty}=0$$

The solution of the equations set (1) with the initial and boundary conditions (2) is searched numerically using the finite difference method of second order accuracy with splitting for physical parameters on spaced "chessboard" grid for spatial derivatives. The method was realized in the coordinate system connected to a sloping plate (see Fig.1) in order to avoid the known difficulties arising in finite difference approximations with a generation of fine meshes at sloping surfaces and discontinuous interfaces, such as abrupt changes in geometry or fluid properties.

With the purpose of verification and outlook to consider more complicated geometries we also solve the posed problem using finite volume method, which nowadays is the most popular numerical approach. The method was realized in the frame of independently developed solvers of the OpenFOAM package, which is free and open source software for the development of customized numerical solvers for computational fluid dynamics. The data obtained by the both approaches were compared with each other for controlling of numerical errors and checking on validity of physical results.

The calculations of the problems were run in parallel regime on SRCC MSU and JSCC RAS supercomputer complexes using the public domain openMPI implementation of the standard message passing interface (MPI). The method of parallel computing is known as domain decomposition, in which the geometry and associated fields are broken into pieces and allocated to separate processors for solution.

The numerical data were post-processed using the graphical interface, ParaView, and the program package, Origin, with the application of a high-resolution method of polychromatic contour map construction. Such an approach allows a programmer to extract both qualitative and quantitative information from the constructed fields for different physical parameters. The colour information on a field structure between neighboring isolines is presented in the form of a continuous gradation spectrum ranging from white to green (light-gray) colours for positive values of a chosen physical variable and from blue (dark-gray) to white colours for negative ones [23].

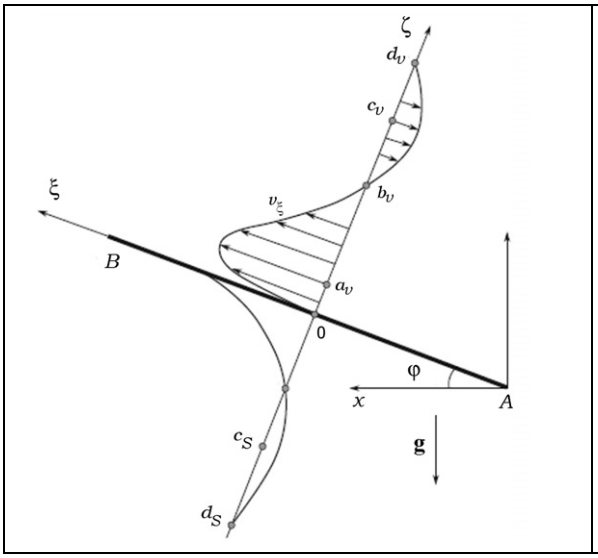

Fig.1. Laboratory and local coordinate systems and profiles of the longitudinal velocity component and salinity perturbation in the center of a sloping plate.

3. Computational results and discussion

The process of a DIF formation on a sloping plate is illustrated by the example of evolution through time of the fields of velocity components presented at Fig.2. Interruption of diffusion flux by the motionless plate results in salt accumulation at its lower side and salt deficiency at the upper one that subsequently leads to a horizontal nonuniformity of density distribution. Arising buoyancy forces generate compensating flows in the up- and downward directions along the upper and the lower sides of the plate, correspondingly. At the initial stage of the flow formation longitudinal component of velocity is uniformly distributed along the plate surface (Fig.2(a)), while its normal component is nonzero only in the vicinity of the plate edges (Fig.2(d)).

The processes of basic jet flow separation at one edge of the plate and drawing of the surrounding fluid to the plate at its opposite edge lead to formation of rather large closed circulating cells adjoined directly to the basic jet flows (Fig.2(b)). The values of normal velocity component at the opposite edges take the different signs, indicating the anticyclonic direction of rotation in these cells (Fig.2(e)). The action of buoyancy forces effects the outgoing fluid the more the greater distance from the edges, thus determining horizontal orientation of the flow away from the obstacle.

Gradually the velocity distribution patterns take a cellular-like form when each flow is followed by the corresponding backflow, that is typical for dissipative gravitational waves (Fig.2(c),(f)). Intensities of both the basic jet flows and the secondary ones increase in time, while the rate of change decreases the faster the closer to the stationary regime of the flow.

The clearest representation of DIFs can be given by stream lines, which are shown in Fig.3 for different slope angles of the plate to the horizon. The steady flow patterns around a horizontal plate, which simulates the central section of an impermeable obstacle with an arbitrary shape, consists of a four-level sequence of horizontally oriented circulating cells, which are located symmetrically relative to the plate's horizon and its central vertical plane (Fig.3(a)). The contacting cells circulate in the opposite directions and are mutually coordinated in contrast to the case of thermal convection where circulations in adjacent cells have the same signs.

Such investigations are of great scientific and practical interest since both the stationary and non-stationary analytical solutions of the problem are constructed only in the approximation of an infinite plane and they cease to work when the slope angle of the plane approaches zero [1 – 3].

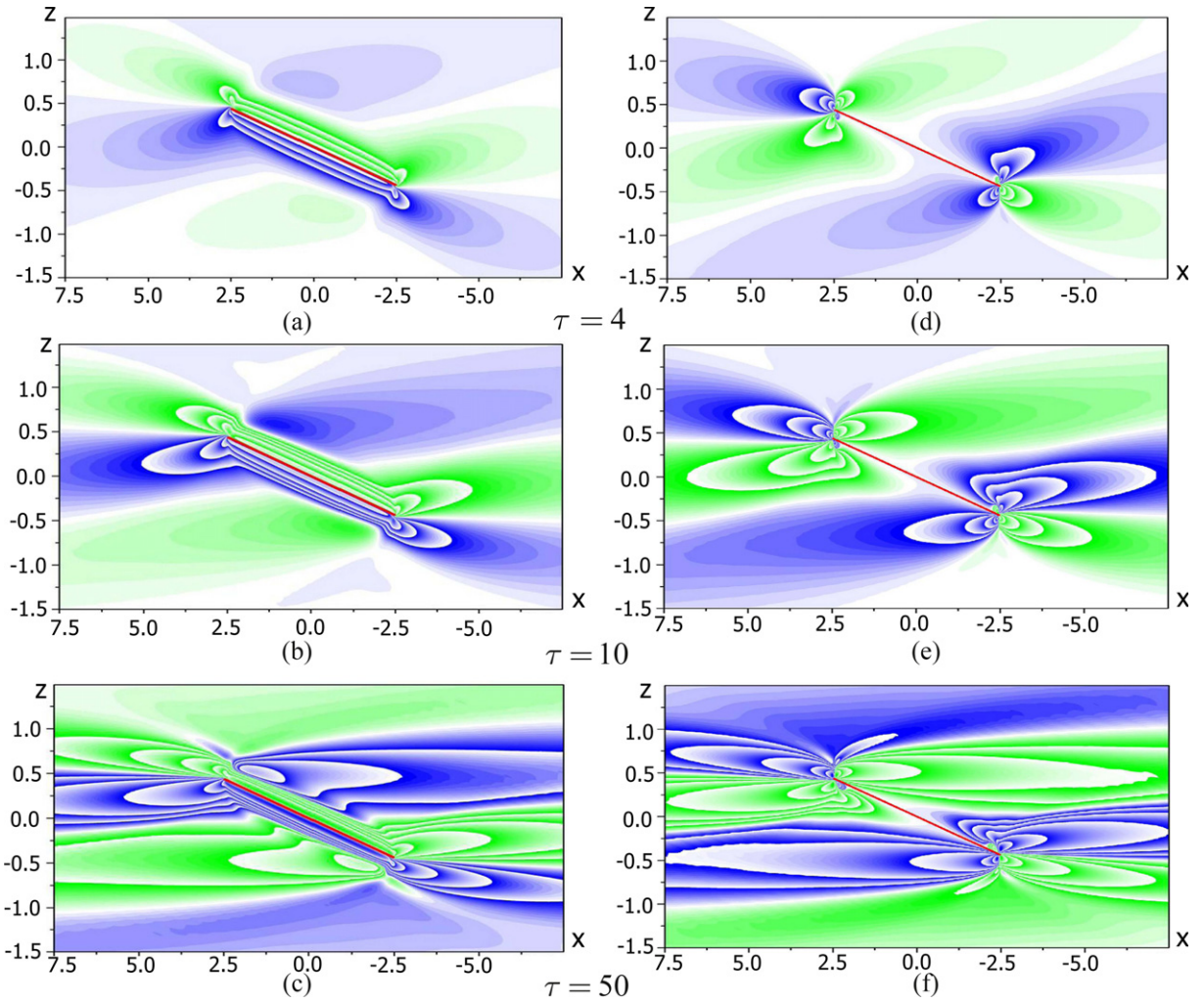

Fig. 2. Patterns of flow evolution through time. (a) – (c) longitudinal velocity component. (d) – (f) normal velocity component. $N = 1.26\ s^{-1}$, $L = 5$ cm, $\varphi = 10^{\circ}$.

Even the smallest deviation from the horizontal position of the plate leads to flow symmetry breakdown and formation of new circulation systems including unidirectional jet flows along the both sides of the sloping plate and secondary compensating circulating flows (Fig.3(b)). A single circulation system is formed around the plate surface, where fluid flows down along the lower side of the plate, turns around in the large cell adjoining the right edge, flows up along the upper side of the plate, turns left and closes in the down-slope jet flow. At small slope angles two types of flows co-exist near the obstacle, some fluid remaining closed in the vortex flow directly near the plate edges and another part accomplishing cyclonic circulating motion around the whole surface of the obstacle.

Further increase in slope angle leads to formation of uniform distribution of the basic jet flows along virtually the whole plate's length excluding rather small regions near the plate edges. The amount of blocked fluid near the edges decrease and the basic jet flows split into two oppositely oriented jets when separating from the surface, thus leading to a general enlargement of the basic cyclonic circulating system (Fig.3(c)). For the values of slope

angles greater than 20 degree, new complicated vortex systems begin to arise near the plate edges within the circulating cells adjacent directly to the basic jet flows (Fig.3(d)). The greater slope angle the longer these vortex structures, which gradually take a wing-shaped form and the general flow structure begin to symmetrize relative to the plate's plane. At the external border of the adjacent circulating cells, additional non-uniformities are revealed, whose regularity directly correlates with the value of buoyancy period N_b.

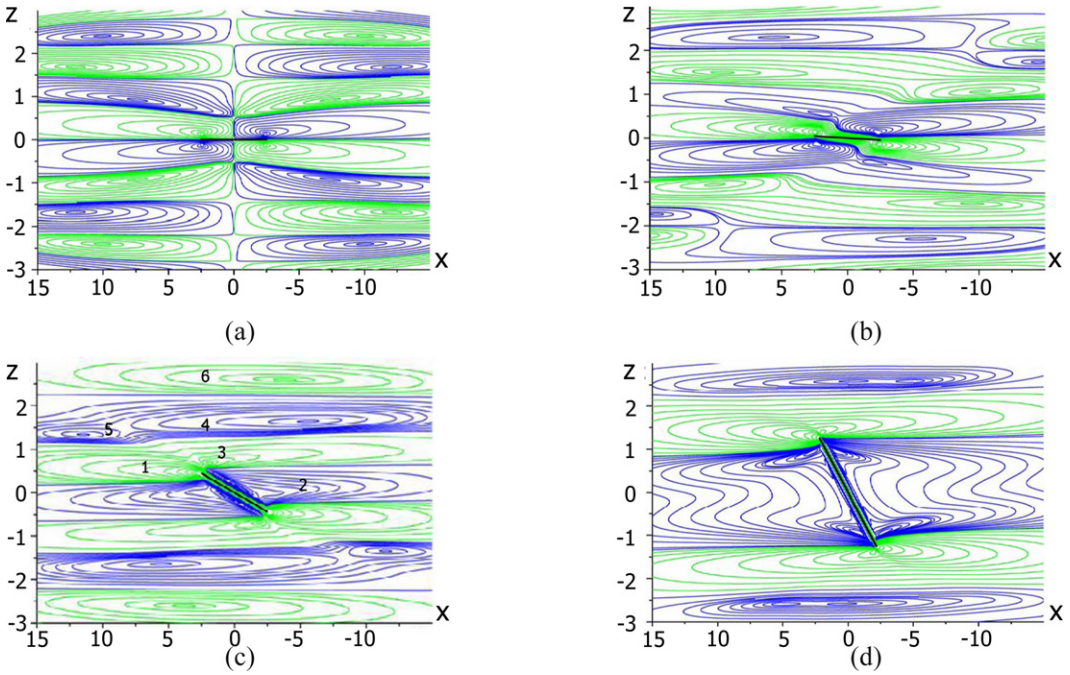

Fig. 3. The patterns of stream lines of diffusion induced flow on a sloping strip.
(a) $\varphi = 0^\circ$. (b) $\varphi = 1^\circ$. (c) $\varphi = 10^\circ$. (d) $\varphi = 30^\circ$. $N = 1.26\, s^{-1}$, $L = 5$ cm, $\tau = 50$.

The patterns of stream lines are supplemented with patterns of distributions of different physical variables, which are presented in Fig.4 including fields of salinity perturbation, pressure, baroclinic generation of vorticity rate and mechanical energy dissipation rate. As it's well seen from the pictures an each field has its own a unique structure, that indicates the complexity of internal structure even of such a slow flow arising due to a nonuniformity of molecular flux of the stratifying agent.

The salinity perturbation field (Fig.4(a)) demonstrates thin layers of salinity deficiency over the plate and its excess under the obstacle due to breaking of the diffusion flux of the stratifying agent by the impermeable obstacle. At a distance from the surface, the field structure changes to be non-monotone, i.e. the thin layers adjoining the plate are followed by streaks with salinity excess over the plate and deficiency under it. Such a structure is typical for zero-frequency waves which are observed near the boundaries of convective flows.

The pattern of the pressure perturbation field, which is presented in Fig.4(b), clearly demonstrates the intensive pressure drop areas in the form of thin dark-gray streaks along the plate's sides and the extensive horizontal regions adjoining the lower edge from the right and to the upper edge from the left. Their appearance is due to the inertia of jets flowing away from the plate and the surrounding fluid flowing towards the obstacle in the areas of up and down-slope jet formation. The separation of jet flows from the surface at the plate's edges leads to the formation of typical horizontal streaky structures and the generation of momentum of the forces turning a sloping plate to the stable horizontal position [20].

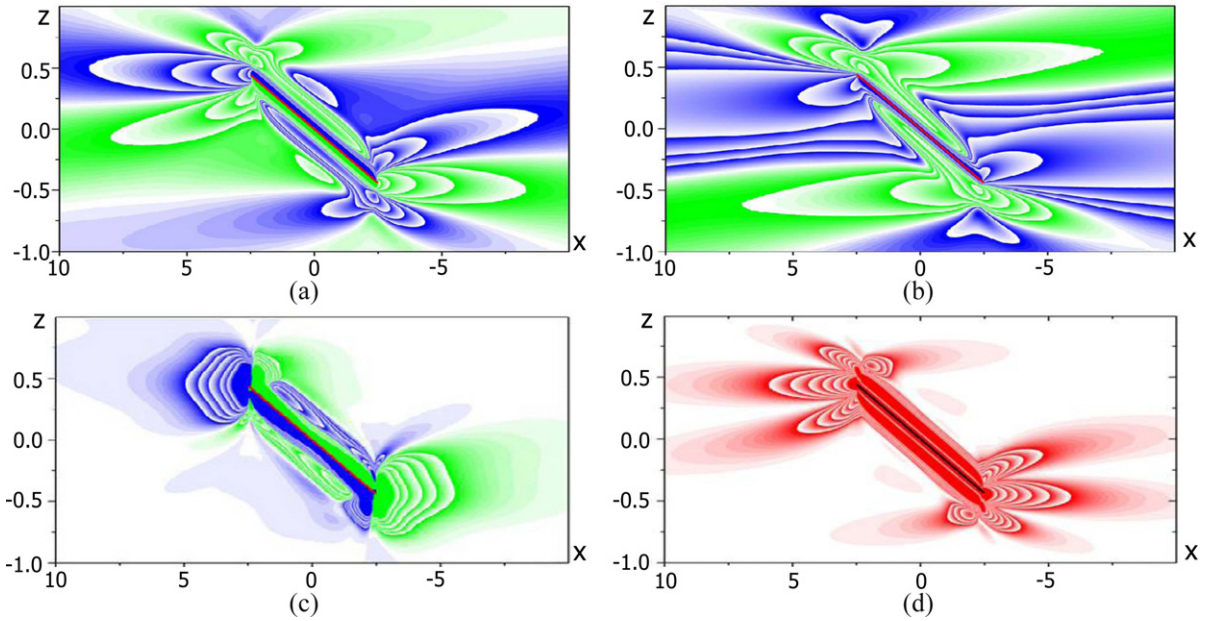

Fig. 4. The fields of different physical variables of diffusion-induced flow on a sloping plate. (a) pressure. (b) salinity perturbation. (c) baroclinic generation of vorticity rate. (d) mechanical energy dissipation rate. $N = 1.26\,s^{-1}$, $L = 5$ cm, $\varphi = 10°$.

The field of baroclinic generation rate of vorticity $\dot{\Omega}$ presented in Fig.4(c) is nonzero in a broad area. A distinguishing feature of this field is a clearness and vertical position of frontiers, which divide the areas of generation and loss of vorticity in the flow. The main particular feature of the mechanical energy dissipation rate field, which is calculated in the laboratory coordinate system and presented in Fig.4(d), is that its maximums are located along the plate line at some distance from the surface while the disturbances in the far flow field are generated mainly by the plate edges.

Comparison of the images in Fig.4 shows significant differences in localization and geometry of the fields of different physical variables and demonstrates a number of particular features indicating an important role of vorticity generation processes out of the flow region adjoining directly to the plate and complicated irregular structure of the field of mechanical energy dissipation rate relative to the large-scale structure of circulating cells.

The flow characteristics are influenced essentially by the fluid properties, that is clearly demonstrated in Fig.5 in the form of tangential velocity profiles for different values of the molecular diffusivity and the kinematic viscosity. An increase in values of the coefficients leads to a proportional growth of spatial wall-normal scales of velocity and salinity perturbations near the surface. Intensity of the along-slope jet flow grows with increase in the value of the diffusivity while decreasing with growth of the molecular viscosity.

The calculation results are compared with the stationary analytical solutions for infinite sloping plane marked in Fig.5 with dotted lines in a wide variation range of the viscosity and diffusivity coefficients. The numerical and theoretical profiles are in an agreement across almost the whole along-slope jet flow but there are some noticeable differences in the backflow especially at large values of κ_S coefficient due to the influence of the plate edges since in the calculations obstacle.

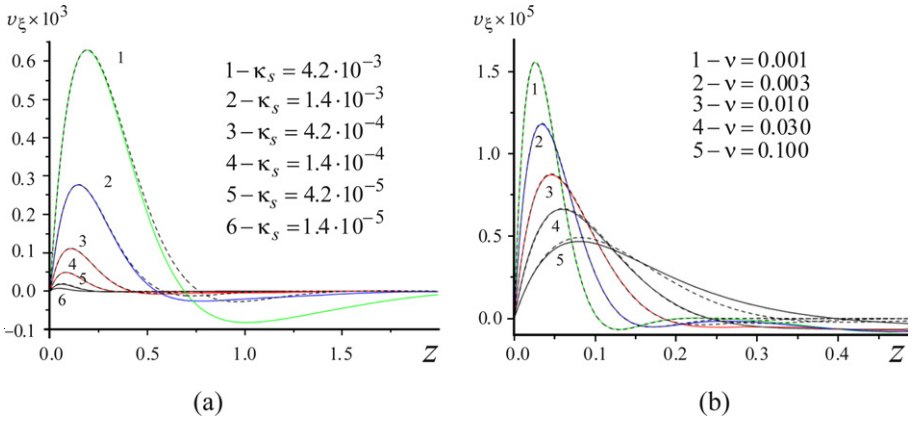

Fig. 5. Profiles of longitudinal velocity component in the center of the plate in comparison with the analytical evaluations in the infinite plane approximation (dotted lines). (a) for different values of diffusion coefficient ($\kappa_S = 1.41 \div 420\times10^{-5}$ cm^2/s (curves 1 – 6)). (b) for different values of kinematic viscosity coefficient ($\nu = 0.001 \div 0.1$ cm^2/s (curves 1 – 5)). $N = 1.26\, s^{-1}$, $L = 5$ cm, $\varphi = 10°$.

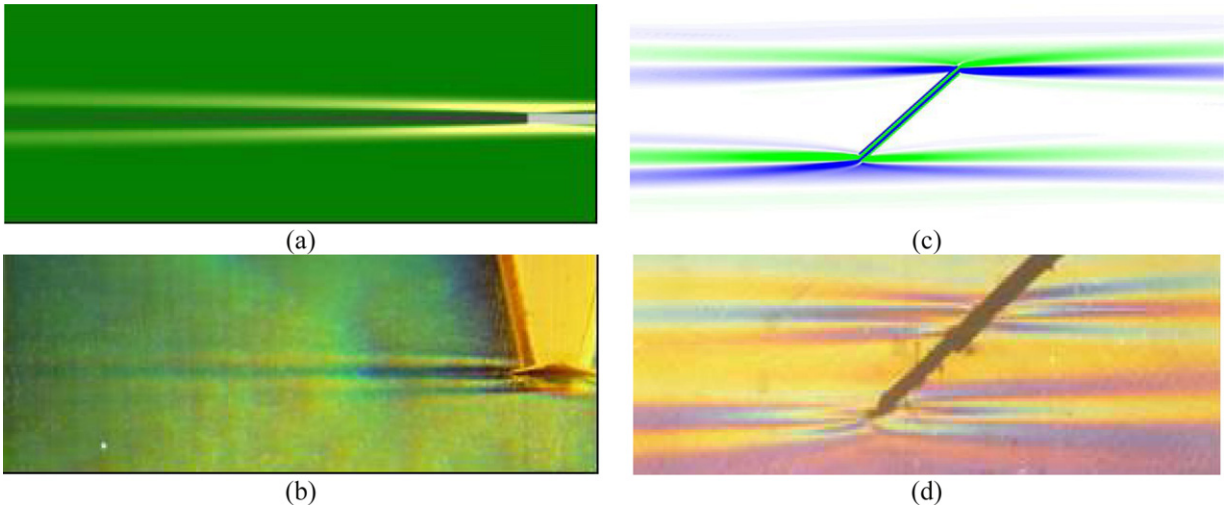

Fig. 6. Comparison of computational and laboratory data on DIF around impermeable horizontal and sloping plates. (a, c) calculated flow patterns. (b, d) images of Schlieren visualization.

The salt concentration near the impermeable surface grows in absolute values with increase of either κ_S or ν coefficients but there is a threshold value of the viscosity above which salinity stops changing. For the considered case of the molecular diffusivity $\kappa_S = 1.41\cdot10^{-5}$ cm^2/s and the characteristic fluid density $\rho_0 = 10^{-3}$ kg/cm^3, the critical value of viscosity coefficient is about $\nu_{cr} \approx 0.02$ cm^2/s. For small values of the dissipation coefficients the total thickness of along-slope jet flows is about twice greater than the thickness of density perturbation variability area but this rule is slightly broken in the case of large values of the coefficients κ_S and ν.

The calculated fields of density gradient $\nabla\rho$ for DIFs on a plate, in which both the large-scale components commensurable with the plate length and thin interfaces with typical scales, $\delta_N^\nu = \sqrt{\nu/N}$ and

$\delta_N^{\kappa_S} = \sqrt{\kappa_S / N}$, are in a good agreement at large times with the Schlieren visualization patterns of refraction ratio around motionless horizontal and sloping plates in the laboratory tank [24]. In both the calculated and Schlieren images the extensive horizontal streaky structures are clearly observed being attached directly to the plate's edges, which serve as sources of dissipative-gravity waves (Fig.6). The length of the visualized streaky structures grows with increase in sensitivity of the registration method in the laboratory experiments. DIFs always exist in a stratified medium at an arbitrary orientation of an impermeable obstacle and non-exist in homogeneous fluid.

Acknowledgements

The work was supported by the Russian Foundation for Basic Research grant # 11-07-90904-mob_sng_st. Experiments were performed on facilities USU "HPC IPMech RAS" under support of Ministry of Education and Science RF (State contract No. 16.518.11.7059).

References

[1] Prandtl L. *The Essentials of Fluid Dynamics*. London: Blackie and Son; 1952.
[2] Phillips OM. On flows induced by diffusion in a stably stratified fluid. *Deep-Sea Res.* 1970;**17**:435 – 43.
[3] Wunsh C. On oceanic boundary mixing. *Deep-Sea Res.* 1970;**17**:293 – 301.
[4] Huppert HE, Turner JS. On melting icebergs. *Nature* 1978;**271**:46 – 8.
[5] Gurnis M. Large-scale mantle convection and the aggregation and dispersal of supercontinents. *Nature* 1988;**332**:695 – 9.
[6] Pawlak GP, Armi L. Mixing and entrainment in developing stratified currents. *J. Fluid Mech.* 2000;**424**:45 – 73.
[7] Ledwell JR, Montgomery ET, Polzin KL, St Laurent LC, Schmitt RW, Toole JM. Evidence for enhanced mixing over rough topography in the abyssal ocean. *Nature* 2000;**403**:179 – 82.
[8] Oerlemans J, Grisogono B. Glacier winds and parameterization of the related heat fluxes. *Tellus* 2002;**54A**:440 – 52.
[9] Thompson L, Johnson GC. Abyssal currents generated by diffusion and geothermal heating over rises. *Deep-Sea Res.* 1996;**43**(2):193 – 211.
[10] Allshouse MR, Barad MF, Peacock T. Propulsion generated by diffusion-driven flow. *Nature Phys.* 2010;**6**:516 – 9.
[11] Page MA. Propelled by diffusion. *Nature Phys.* 2010;**6**:486 – 7.
[12] MacIntyre S, Alldredge AL, Gotschalk CC. Accumulation of marine snow at density discontinuities in the water column. *Limnol. Oceanogr.* 1995;**40**:449 – 68.
[13] Hoyal DCJD, Bursik MI, Atkinson JF. Settling-driven convection: a mechanism of sedimentation from stratified fluids. *Geophys. Res.* 1999;**104**:7953 – 66.
[14] Linden PF, Weber JE. The formation of layers in a double-diffusive system with a sloping boundary. *J. Fluid Mech.* 1977;**81**:757 – 73.
[15] Kistovich AV, Chashechkin YuD. The structure of transient boundary flow along an inclined plane in a continuously stratified medium. *Appl. Math. Mech.* 1993;**57–54**:633 – 9.
[16] Page MA, Johnson ER. Steady nonlinear diffusion-driven flow. *J. Fluid Mech.* 2009;**629**:299 – 309.
[17] Woods AW. Boundary-driven mixing. *J. Fluid Mech.* 1991;**226**:625 – 54.
[18] Zyryanov VN, Lapina LE. Hillside flows in oceans, lakes and reservoirs due to diffusion effects. *Water Resour.* 2012;**39**(3):292 – 303 (in Russian).
[19] Burkholder B, Shapiro A, Fedorovich E. Katabatic flow induced by a cross-slope band of surface cooling. *Acta Geophys.* 2009;**57**:923 – 49.
[20] Chashechkin YuD, Zagumennyi YaV. Structure of diffusion-induced flow on an inclined plate. *Doklady Physics* 2012;**57**(5):210 – 6.
[21] Zagumennyi IaV. Flows induced by breaking of substance diffusion flux on topography. *Colloquium Euromech Proceedings on Vortices and Waves:Identifications and Mutual Influences,* Moscow, Russia; June 2011, p. 94 – 96.
[22] Baydulov VG, Matyushin PV, Chashechkin YuD. Structure of a diffusion-induced flow near a sphere in a continuously stratified fluid. *Doklady Physics* 2005;**50**(4)**:**195 – 9.
[23] Chashechkin YuD, Bardakov RN, Zagumennyi YaV. Numerical analysis and visualization of fine structures of the fields of two-dimensional internal waves. *Phys. Oceanogr.* 2011;**20**(6)**:**397 – 409.
[24] Chashechkin YuD. Schlieren visualization of a stratified flow around a cylinder. *J. Visualiz.* 1999;**1**(4):345 – 54.